Nanoscale Research Letters
a SpringerOpen Journal

NANO EXPRESS   **Open Access**

Cellulose-lanthanum hydroxide nanocomposite as a selective marker for detection of toxic copper

Hadi M Marwani[1,2*], Mazhar Ullah Lodhi[1], Sher Bahadar Khan[2] and Abdullah M Asiri[1,2]

Abstract

In this current report, a simple, reliable, and rapid method based on modifying the cellulose surface by doping it with different percentages of lanthanum hydroxide (i.e., 1% $La(OH)_3$-cellulose (LC), 5% $La(OH)_3$-cellulose (LC2), and 10% $La(OH)_3$-cellulose (LC3)) was proposed as a selective marker for detection of copper (Cu(II)) in aqueous medium. Surface properties of the newly modified cellulose phases were confirmed by Fourier transform infrared spectroscopy, field emission scanning electron microscope, energy dispersive X-ray spectroscopy, X-ray diffraction, and X-ray photoelectron spectroscopic analysis. The effect of pH on the adsorption of modified cellulose phases for Cu(II) was evaluated, and LC3 was found to be the most selective for Cu(II) at pH 6.0. Other parameters, influencing the maximum uptake of Cu(II) on LC3, were also investigated for a deeper mechanistic understanding of the adsorption phenomena. Results showed that the adsorption capacity for Cu(II) was improved by 211% on the LC3 phase as compared to diethylaminoethyl cellulose phase after only 2 h contact time. Adsorption isotherm data established that the adsorption process nature was monolayer with a homogeneous adsorbent surface. Results displayed that the adsorption of Cu(II) onto the LC3 phase obeyed a pseudo-second-order kinetic model. Selectivity studies toward eight metal ions, i.e., Cd(II), Co(II), Cr(III), Cr(VI), Cu(II), Fe(III), Ni(II), and Zn(II), were further performed at the optimized pH value. Based on the selectivity study, it was found that Cu(II) is highly selective toward the LC3 phase. Moreover, the efficiency of the proposed method was supported by implementing it to real environmental water samples with adequate results.

Keywords: Nanostructures; Nanocomposite; Cu(II); Modified cellulose phase; Separation; ICP-OES; Batch method

Background

Over the years, copper (Cu(II)) has gain the attention of chemists due to its prohibitive toxicity and nonbiodegradable nature. The elevated concentration of Cu(II) produces severe ecological and public health issues [1,2]. Several methodologies have been evaluated for the separation of Cu(II) in aqueous medium. However, the adsorption technique has proved to be one of the promising solutions due to its simple implementation and economical and effective behavior [3,4]. Currently, some of the available adsorbents have limitations, such as low uptake capacity, long equilibrium, and low selectivity [5]. In order to overcome these weaknesses, some new organic-inorganic hybrid adsorbents, capable of separating heavy metals from the solution, have been established. Several studies have been concentrated on the extraction of Cu(II) by applying amine group functionalized matrices [6-9]. It is well understood that organic functional group modified adsorbents usually exhibit relatively high adsorption capacity and selectivity as compared to unmodified adsorbents [6,10-12].

Different separation techniques, however, are being successfully utilized, for example, liquid-liquid extraction [13], ion exchange [14], coprecipitation [15], cloud point extraction [16], and solid phase extraction (SPE) [17,18]. The conventional methods, such as liquid-liquid extraction and coprecipitation, require excess amount of organic solvents with high purity that could be harmful to living organisms and cause environmental pollution. On the other hand, the SPE method proved to be a more efficient technique when it comes to the exposure and usage of solvents, extraction time, and disposal cost. Presently, this recognition of SPE leads to the appearance of several adsorbents with the goal of succeeding a

* Correspondence: hmarwani@kau.edu.sa
[1]Department of Chemistry, Faculty of Science, King Abdulaziz University, P.O. Box 80203, Jeddah 21589, Saudi Arabia
[2]Center of Excellence for Advanced Materials Research (CEAMR), King Abdulaziz University, P.O. Box 80203, Jeddah 21589, Saudi Arabia

Springer

selective separation of the analytes, for instance, alumina [19], C18 [20], molecular imprinted polymers [21], cellulose [22], silica gel [23], and activated carbon [24,25].

Cellulose is considered to be one of the highly abundant naturally existing polymers in the world. This comprises repeating units of β-D-glucopyranose, covalently linked with OH group of C4 and C1 carbon atoms [26-28]. Naturally occurring cellulose shows less adsorption capacity and physical stability due to the steric hindrance offered by three hydroxyl groups with the same ring. Moreover, these hydroxyl moieties are chemically unreactive as the polymer matrix contains crystalline regions [27,29]. In order to develop adsorption capacity and structural stability of natural cellulose, modifications were employed in the matrix by means of chemical reactions, such as halogenation, etherification, esterification, and oxidation. Such modified matrices were found to be capable of separating heavy metal ions from aqueous solutions [27]. The cellulose beads when treated mainly with 2-(diethylamino) ethyl chloride hydrochloride along with some other treatments produced diethylaminoethyl cellulose [30]. Recently, we have also developed some surface modified cellulose adsorbents for the selective separation of Ni(II) and Cr(VI) ions [31,32].

In order to monitor metal ionic species in the environment, the development of rapid, simple, and proficient approach has gain an interest. Different approaches were employed for the determination of metal ions in aqueous medium, namely atomic absorption spectrometry (AAS) [33], inductively coupled plasma-mass spectrometry (ICP-MS) and inductively coupled plasma-optical emission spectrometry (ICP-OES) [34-36], anodic stripping voltammetry [37], and ion chromatography [38]. Despite immense enhancement in selectivity and sensitivity of state-of-the-art instruments, there is still a vital need for improvement in selective separation of chemical species of interest prior to their determination; in particular, the concentration of such analytes is frequently low in complex matrices. Moreover, a cleanup step is frequently needed because of high level of other constituents accompanying the analyte.

Current study emphasizes the development of new cellulose-based adsorbents by surface modification. Lanthanum hydroxide was doped with cellulose with a proportion of 1%, 5%, and 10% [i.e., 1% La(OH)$_3$-cellulose (LC), 5% La(OH)$_3$-cellulose (LC2), and 10% La(OH)$_3$-cellulose (LC3)]. Additionally, the effectiveness of nanocomposites was investigated as a potential adsorbent for a selective extraction of Cu(II) ion prior to its determination by ICP-OES. Several parameters were evaluated in order to acquire the optimum condition for Cu(II) extraction. The pH effect on Cu(II) adsorption was investigated and optimized for the best modified cellulose phase (LC3). In order to understand the mechanism of

Cu(II) adsorption, other parameters controlling the maximum uptake of Cu(II) on LC3 was studied at the optimum pH 6.0. Furthermore, adsorption data was modeled by Freundlich and Langmuir adsorption isotherms. The kinetics of adsorption was evaluated by employing pseudo-first- and second-order kinetic models. At optimized pH, selectivity was also scrutinized for other metal ion, including Cd(II), Co(II), Cr(III), Cr(VI), Fe(III), Ni(II), and Zn(II). This study revealed that LC3 was the most selective toward Cu(II) in comparison to other metal ions. Ultimately, the proposed method was further validated by analysis of real environmental water samples.

Methods
Chemicals and reagents
Diethylaminoethyl (DEAE) cellulose, lanthanum chloride, and ethanol were purchased from Sigma-Aldrich (Milwaukee, WI, USA). Stock standard solutions of 1,000 mgL^{-1} Cd(II), Co(II), Cu(II),Cr(III), Cr(VI), Fe(III), Ni(II), and Zn(II) were obtained from Sigma-Aldrich (Milwaukee, WI, USA). All utilized reagents were of high purity and of analytical reagent grade, whereas double-distilled deionized water was used throughout the experiments.

Preparation of the new solid phase extractor based on DEAE cellulose
Different amounts of DEAE cellulose (99%, 95%, and 90%) were first mixed with distilled deionized water. Various portions of lanthanum chloride (1%, 5%, and 10%) were then dissolved in distilled deionized water and mixed with DEAE cellulose water suspensions. All solutions were adjusted to pH 10.0 by a dropwise addition of 0.1-M NaOH. Mixtures were then allowed to stir at 60°C for 24 h. Mixtures were filtered, washed with ethanol twice and 18.2 MΩ cm distilled deionized water, and dried in oven at 80°C for 5 h to obtain LC, LC2, and LC3 nanocomposites.

Samples preparation and procedure
Stock standard solutions of Cd(II), Co(II), Cu(II),Cr(III), Cr(VI), Fe(III), Ni(II), Pb(II), and Zn(II) ions were prepared in 18.2 MΩ cm distilled deionized water and stored in the refrigerator at 4°C. The environmental samples were collected from seawater, wastewater, tap water, and ground water from Jeddah region at Saudi Arabia.

Effect of pH
The effect of pH on the adsorption of Cu(II) ion onto n% La(OH)$_3$ DEAE cellulose was investigated. Standard solutions of 5.0 mgL^{-1} Cu(II) were adjusted to pH values ranging from 1.0 to 8.0 with appropriate buffer solutions, i.e., HCl/KCl buffer for pH 1.0 and 2.0, acetate buffer for pH 3.0 to 5.0, and KH$_2$PO$_4$/NaOH buffer for pH 6.0 to 8.0. Each solution was individually mixed with 25.0 mg of

modified cellulose phases (LC, LC2, or LC3) and unmodified DEAE cellulose phase and mechanically shaken for 2 h by a mechanical shaker at 150 rpm and 25°C temperature.

Effect of concentration

To estimate the uptake capacity of Cu(II) under batch conditions, standard solutions of 0, 1, 5, 10, 20, 30, 40, 50, 80, 100, 150, 200, 300, 400, and 500 mgL^{-1} were prepared and adjusted to the optimum pH 6.0 with the buffer solution of KH$_2$PO$_4$/NaOH. Each solution was individually added to 25.0 mg LC3 (or unmodified DEAE cellulose). All mixtures were then allowed to be mechanically shaken for 2 h at 25°C.

Effect of temperature

For the effect of temperature, standard solutions of 5.0 mgL^{-1} Cu(II) were prepared, adjusted to the pH 6.0 as above, and individually mixed with 25.0 mg LC3. Thermodynamic study of the adsorption of LC3 toward Cu(II) was also performed under the same batch conditions at different temperatures (298, 308, 323, and 338 K).

Effect of shaking time

The effect of shaking time on LC3 adsorption for Cu(II) was performed under the same batch conditions as above by given various equilibrium periods (5, 10, 20, 30, 50, 80, 100, and 120 min) and at a concentration of 400 mgL^{-1} of Cu(II).

Selectivity studies

In order to investigate the selectivity of modified cellulose adsorbents toward different metal ions, including Cd(II), Co(II), Cu(II), Cr(III), Cr(VI), Fe(III), Ni(II), Pb (II), and Zn(II), 5 mgL^{-1} of each metal ion solution was individually added to 25.0 mg of modified phases (LC, LC2, or LC3) and unmodified DEAE cellulose separately as well. Mixtures were then allowed to be stirred for 2 h at 25°C under the same batch conditions as above.

Apparatus

The surface morphology of the nanocomposites was investigated by operating a field emission scanning electron microscope (FE-SEM) instrument (JSM-7600 F, JEOL Ltd., Akishima-shi, Japan). Elemental analysis was performed using energy dispersive X-ray spectroscopy (EDS) from JEOL, Japan. X-ray diffraction (XRD) patterns were acquired with X-ray diffractometer (Rigaku X-ray diffractometer, MiniFlex 2, Rigaku, Shibuya-ku, Japan) equipped with Cu-Kα1 radiation (λ = 1.5406 nm) using a generator voltage (40.0 kV) and a generator current (35.0 mA). Data of X-ray photoelectron spectroscopy (XPS) were acquired from Thermo Scientific K-α KA1066 spectrometer (Bonn, Germany). The Al Kα X-ray radiation monochromatic sources were utilized as excitation sources, whereas the size of beam spot was set at 300.0 μm. The fixed analyzer transmission mode was used to record the spectra adjusting pass energy at 200 eV. The scan of spectra was performed at a pressure less than 10^{-8} Torr. Fourier transform infrared (FT-IR) spectroscopic analyses were carried out by using Shimadzu IR 470 spectrophotometer (Shimadzu, Kyoto, Japan) to confirm the formation of newly prepared nanocomposites. The pH measurements were performed on pH meter (inoLab® pH 7200, WTW, Lincolnwood, IL, USA) with absolute accuracy limits at the pH measurement being defined by NIST buffers. A PerkinElmer ICP-OES Optima 4100 DV model (PerkinElmer, Waltham, MA, USA) was applied for the determination of
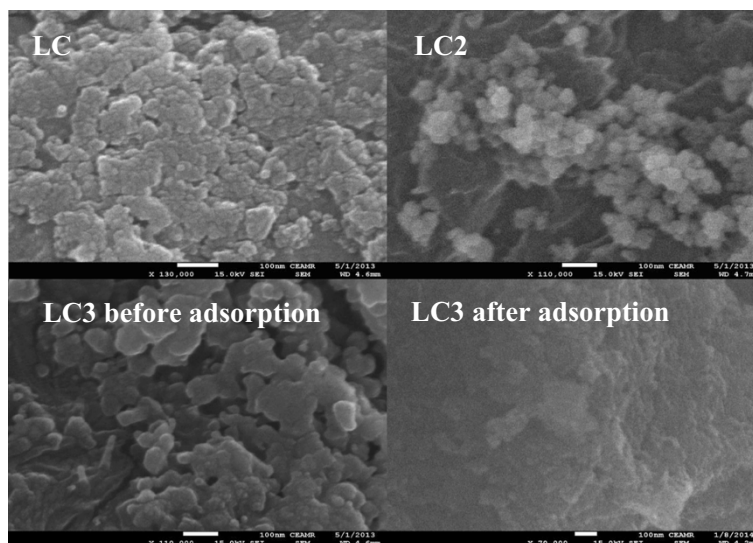
Figure 1 FE-SEM images of modified cellulose phases (LC, LC2, LC3) before adsorption and LC3 after adsorption.

metal ions concentration. The optimization of ICP-OES instrument was performed daily before analysis and operated as recommended by the manufacturers.

The ICP-OES spectrometer was operated with the following parameters: FR power, 1,300 kW; frequency, 27.12 MHz; demountable quartz torch, Ar/Ar/Ar; plasma gas (Ar) flow, 15.0 L min^{-1}; auxiliary gas (Ar) flow, 0.2 L min^{-1}; nebulizer gas (Ar) flow, 0.8 L min^{-1}; nebulizer pressure, 2.4 bar; glass spray chamber according to Scott (Ryton), sample pump flow rate, 1.5 mL min^{-1}; integration time, 3 s; replicates, 3; wavelength range of monochromator, 165 to 460 nm. The concentrations of the metal ions were determined at wavelengths of 226.50 nm for Cd(II), 230.80 nm for Co(II), 267.72 nm for Cr(III and VI), 327.40 nm for Cu(II), 259.94 nm for Fe(III), 231.60 nm for Ni(II), and 202.55 nm for Zn(II).
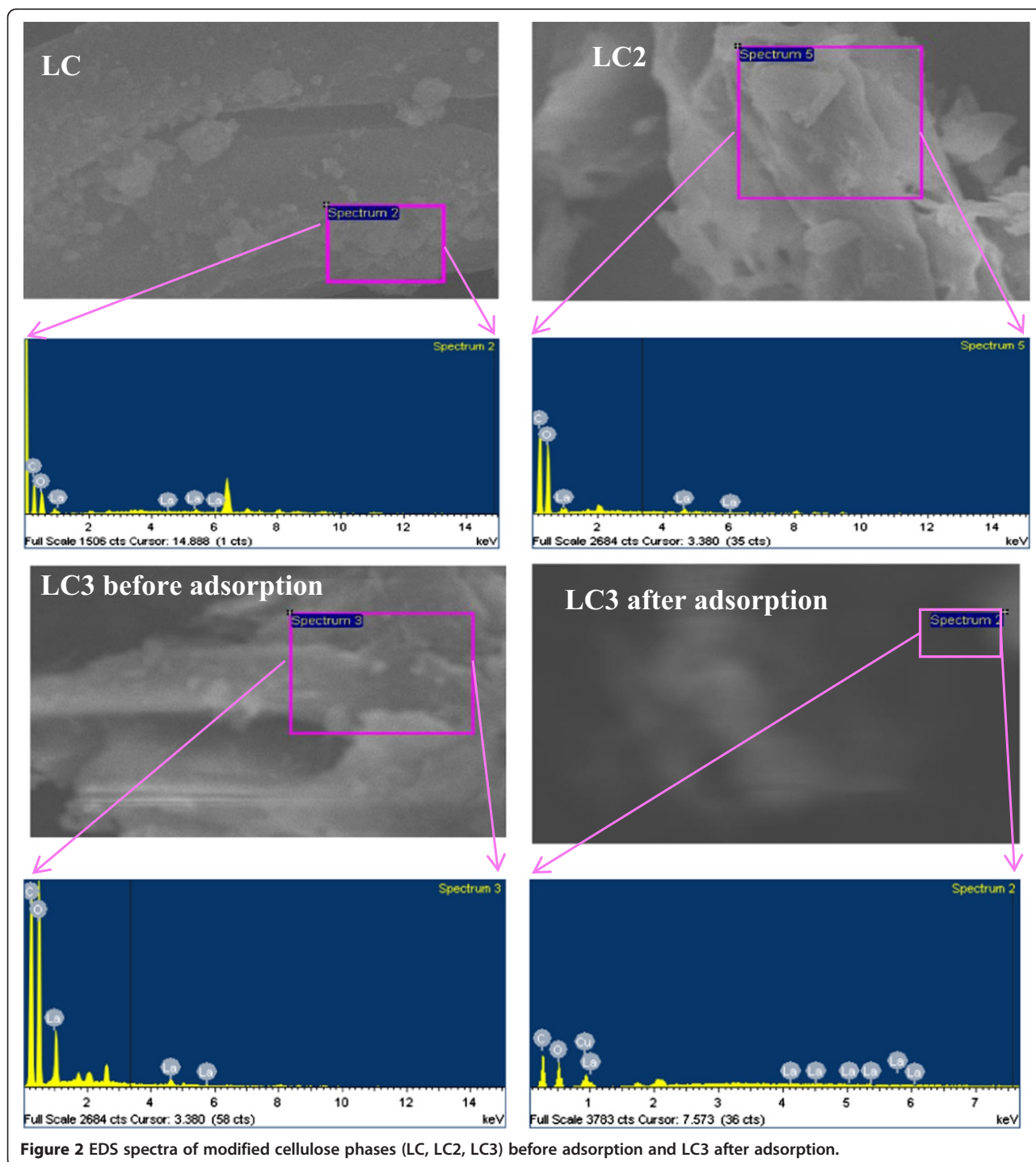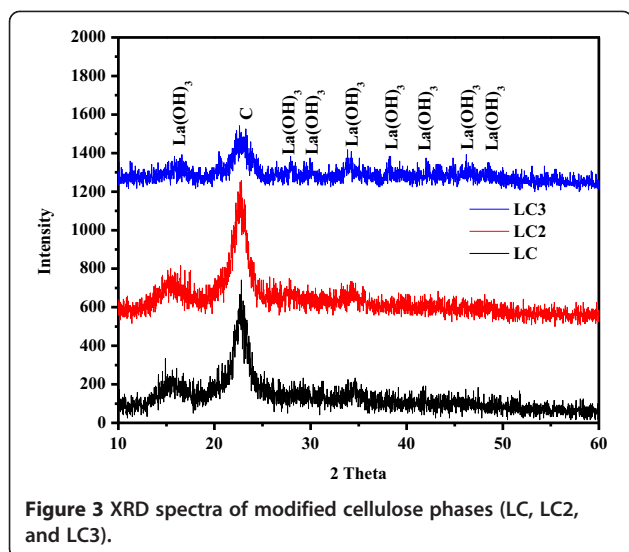

Figure 2 EDS spectra of modified cellulose phases (LC, LC2, LC3) before adsorption and LC3 after adsorption.

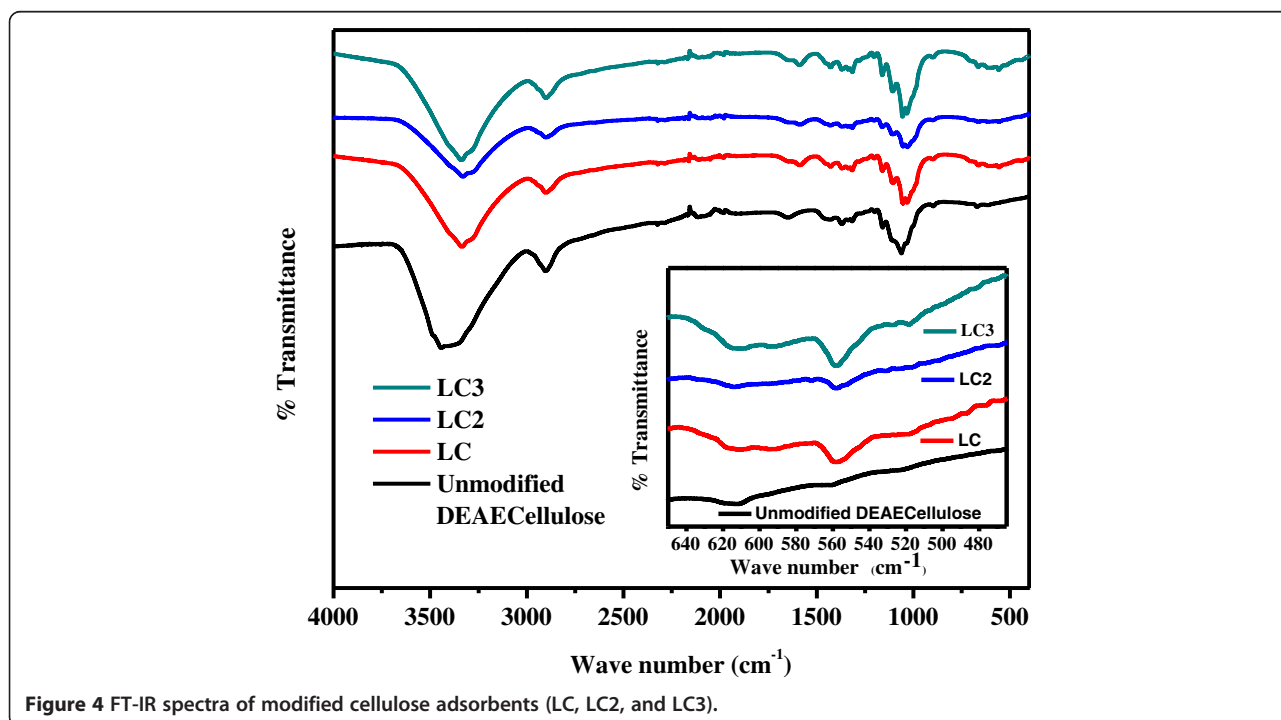**Figure 3** XRD spectra of modified cellulose phases (LC, LC2, and LC3).

## Results and discussion

Characterization

The morphological behavior of synthesized nanocomposites was studied by FE-SEM, as can be depicted in Figure 1. FE-SEM images of nanocomposites are comprised of aggregated nanoparticles with an average particle size of 50 nm. These aggregated nanoparticles are well distributed on the cellulose matrix, proposing that $La(OH)_3$ nanoparticles are dispersed on the cellulose surface. Furthermore, it can be clearly observed from Figure 1 that the size of nanoparticles increases as the

percentage of $La(OH)_3$ doping increases due to aggregation of $La(OH)_3$ on cellulose surface. Conversely, the surface of LC3 matrix was observed with finely adsorbed Cu(II) onto the cellulose surface after the adsorption process. The composition of these nanocomposites was evaluated by EDS spectrum, as shown in Figure 2. In EDS spectra of all modified phases, the peaks, related to carbon, oxygen, and lanthanum at 0.2, 0.5, and 1.0 keV, respectively, are observed without any other impurity peak. This indicates that the synthesized nanocomposites are composed of cellulose and $La(OH)_3$. Adsorption of Cu(II) was also evaluated by EDS by attaining the spectrum of LC3 phase after adsorption. It is of interest to note that a peak at 0.9 keV for Cu(II) is observed in the LC3 spectrum after adsorption.

The purity and crystallinity of synthesized nanocomposites were evaluated using XRD analysis, as displayed in Figure 3. In the XRD pattern of nanocomposites, a hallow peak at 22.0 Å is observed in all the modified cellulose phases (LC, LC2, and LC3), corresponding to amorphous nature of the adsorbents [39]. Moreover, XRD spectra also show several well crystalline peaks at 16.0, 28.0, 30.0, 34.0, 38.37, 42.31, 46.24, and 48.72 Å, describing the growth of $La(OH)_3$ onto the surface of cellulose as reported in the literature [40]. Consequently, the diffraction peaks of all modified cellulose phases confirmed that synthesized products were nanocomposites of cellulose and $La(OH)_3$ nanoparticles. Further, no peaks other than those for cellulose and $La(OH)_3$ were observed in obtained diffraction patterns of modified

Figure 4 FT-IR spectra of modified cellulose adsorbents (LC, LC2, and LC3).
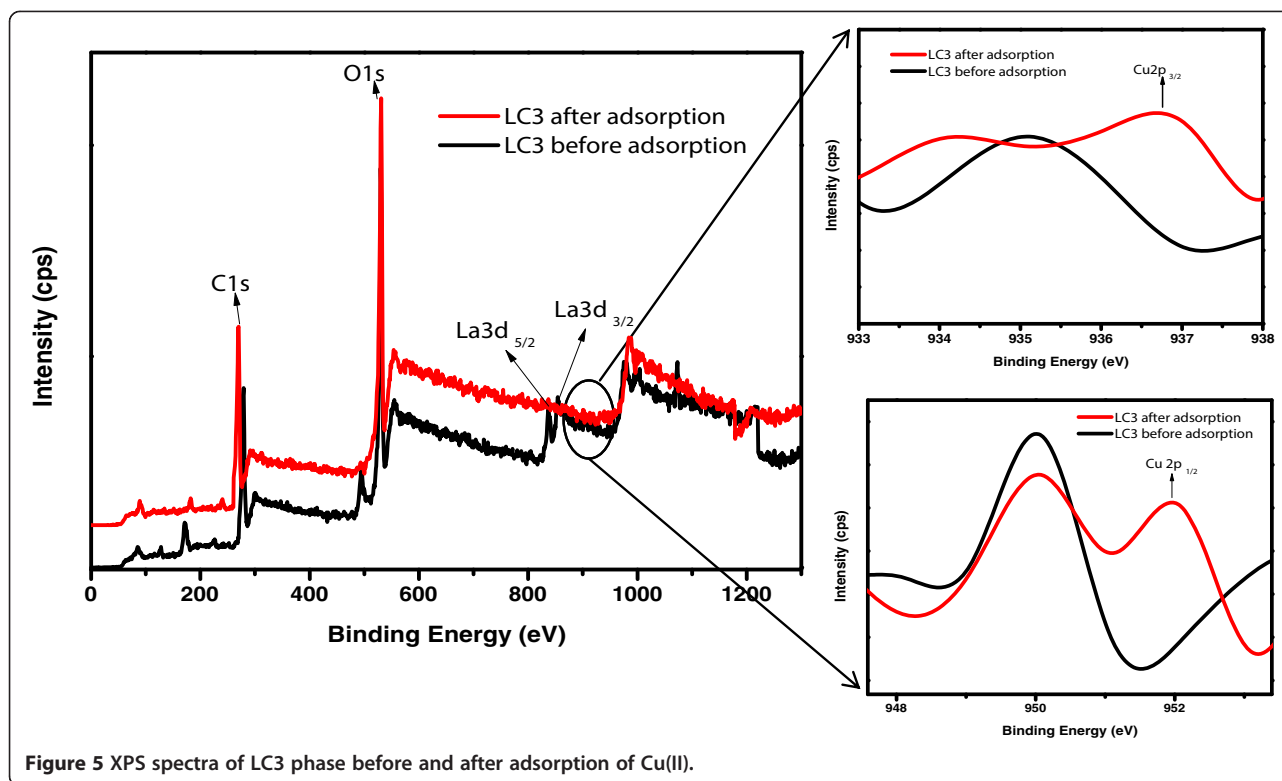
Figure 5 XPS spectra of LC3 phase before and after adsorption of Cu(II).

phases, verifying that the synthesized nanocomposites are composed of cellulose and La(OH)$_3$ [40].
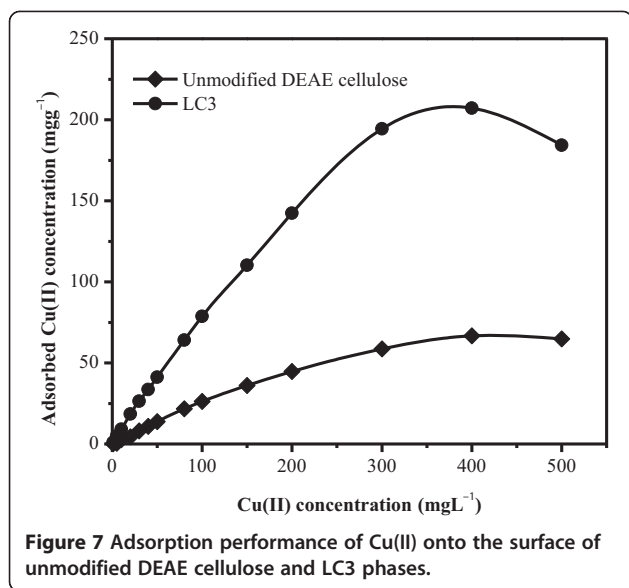
Chemical structures and functional groups presented in synthesized nanocomposites were evaluated by FT-IR spectra, as illustrated in Figure 4. FT-IR spectrum of unmodified DEAE cellulose exhibits a strong absorption band for OH stretching vibration at 3,450 cm^{-1} due to the presence of hydroxyl group. However, the same stretching band for hydroxyl group was shifted to 3,335 cm^{-1} in the spectra of modified cellulose phases (LC, LC2, and LC3). This might be due to an interaction between hydroxyl moiety and doped La(OH)$_3$ onto the surface of cellulose. For unmodified DEAE cellulose, a prominent peak in the FT-IR spectrum at 1,058 cm^{-1}, for C-O stretching band, appeared to shift to a lesser wave number (1,051 cm^{-1}) in modified cellulose phases. FT-IR spectra show peaks at 2,897 and 1,152 cm^{-1}, corresponding to C-H stretching and bending in all the phases of cellulose. Absorption bands at 557 cm^{-1} observed in only modified cellulose phases were due to La-O stretching vibration as depicted in Figure 4. All these characteristic peaks of DEAE cellulose and La(OH)$_3$ detected in the spectrum of nanocomposites confirmed the formation of nanocomposites [40,41].

XPS was performed in order to quantitatively achieve the composition, electronic state, chemical state, and empirical formula of the elements present within a matrix. The XPS spectrum of the material was taken by irradiating it with X-ray beam and obtaining the kinetic energy and number of electrons that escape within 1- to 10-nm region from the material being analyzed. In order to investigate the doping and adsorption phenomena, XPS spectra were taken for best doped cellulose matrix as adsorbent of Cu(II), i.e., LC3, before and after adsorption (Figure 5). For both spectra of LC3 before and after adsorption, the material exhibits peaks at 281.75, 530.96, 834.69, and 851.82 eV, corresponding to C1s, O1s, La3d$_{5/2}$, and La3d$_{3/2}$,
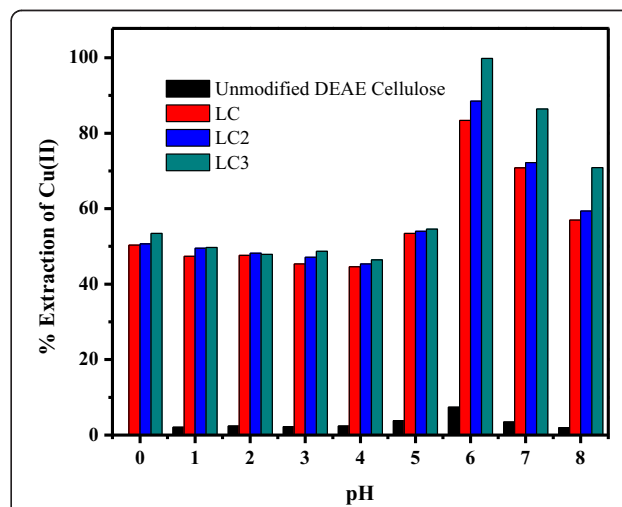
Figure 6 Effect of pH on the adsorption of 5 mgL^{-1} Cu(II). On 25 mg unmodified DEAE cellulose and modified cellulose phases at 25°C.

Figure 7 Adsorption performance of Cu(II) onto the surface of unmodified DEAE cellulose and LC3 phases.

**Figure 9 Adsorption isotherm study of Cu(II) extraction by LC3 at different temperatures.**

respectively. However, new peaks were observed in the LC3 spectrum after adsorption at 936.75 and 951.94 eV, corresponding to $Cu2p_{3/2}$ and $Cu2p_{1/2}$, respectively, as can be depicted in Figure 5. Notably, such peaks of Cu(II) are absent in the spectrum of LC3 before adsorption took place. These characteristic peaks were in agreement with the previous literature [40,42] and further confirmed the formation of doped cellulose matrix with $La(OH)_3$ and adsorption of Cu(II).

Batch method
Effect of pH
The effect of pH was investigated for the selective adsorption of Cu(II) ion onto the modified cellulose phases within the range of 1.0 to 8.0 by applying buffer solutions. The

Figure 8 Effect of contact time on Cu(II) adsorption on 25.0 mg LC3 at pH 6.0 and 25°C.
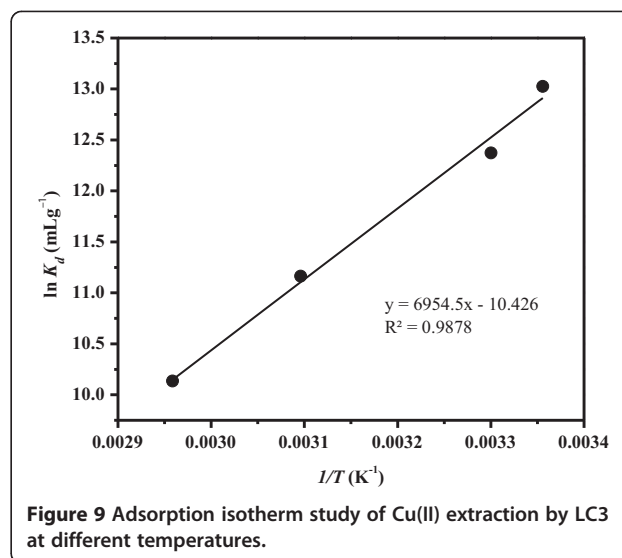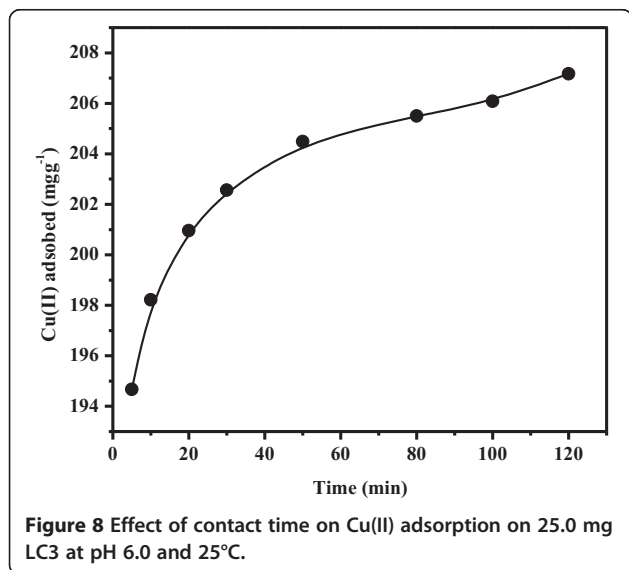
percentage extraction of Cu(II) on unmodified DEAE cellulose was 7.47% at optimum pH 6.0 (Figure 6). However, the percentage extractions for LC, LC2, and LC3 were 83.36%, 88.48%, and 99.78%, respectively. Hence, phase LC3 displayed maximum efficiency for the extraction of Cu (II) among all other modified phases. Although the difference of extraction between the unmodified and modified cellulose matrix was enormous, all phases displayed their maximum extraction at pH 6.0 (Figure 6). At lower pH value, new proton acceptor centers are created and may be competed with metal ions adsorption on binding sites of all phases, resulting in the low adsorption of Cu(II) [43]. However, the highest percentage of Cu(II) extraction (99.78%) at pH 6.0 with LC3 phase can be attributed to highest content of negatively charged sites presented on LC3 phase at this specific pH value and as a result of doping the highest content (10%) of $La(OH)_3$ on DEAE cellulose surface. These negatively charged sites/centers are able to easily bind with the positively charged Cu(II) ions through electrostatic attraction at pH 6.0. It was noticed that adsorption was further decreased at pH greater than 6.0. This may be ascribed to the precipitation of heavy metal ions above pH 6.0 leading to the reduction of the metal ions in the solution [44].

Adsorption capacity
Adsorption capacity of Cu(II) on LC3 was estimated by varying amounts (0 to 500 mgL^{-1}) of Cu(II) and individually mixing them with 25.0 mg LC3 at pH 6.0 under

Table 1 Thermodynamic parameters associated with the adsorption of Cu(II) on LC3 phase

$\Delta H°$ ($kJmol^{-1}$)	$\Delta S°$ ($Jmol^{-1} K^{-1}$)	$\Delta G°$ ($kJmol^{-1}$)			
		$T = 298$ K	$T = 303$ K	$T = 323$ K	$T = 338$ K
−57.82	−86.68	−32.27	−31.17	−29.98	−28.48
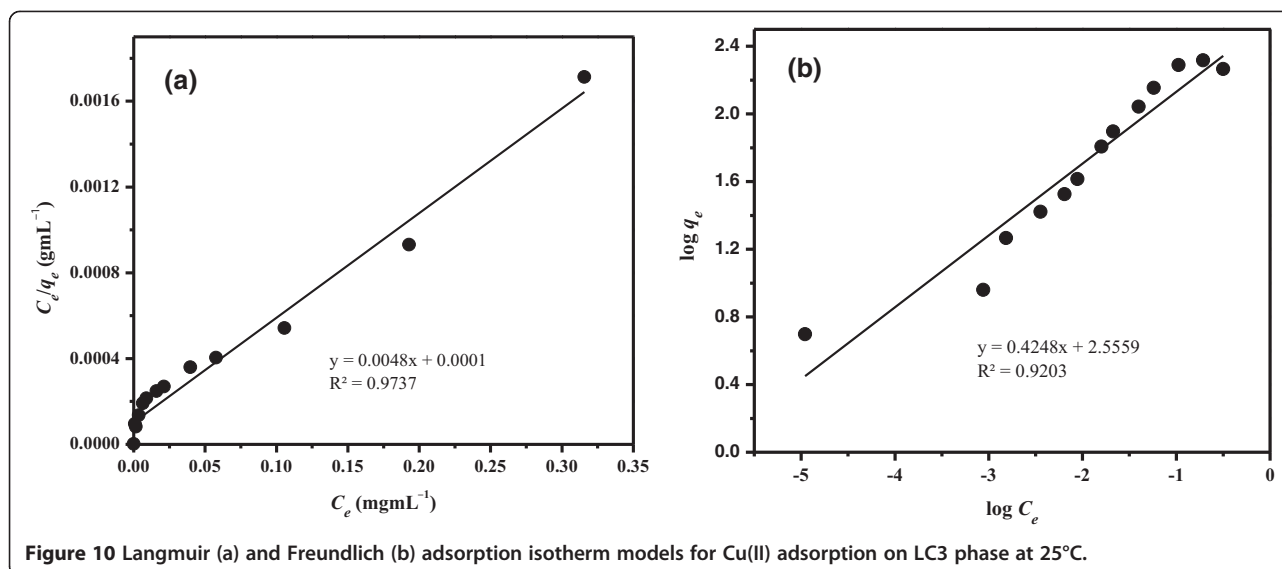
Figure 10 Langmuir (a) and Freundlich (b) adsorption isotherm models for Cu(II) adsorption on LC3 phase at 25°C.

batch procedure. Uptake capacities of unmodified DEAE cellulose and LC3 for Cu(II) were determined by plotting a breakthrough curve between concentration (mgL^{-1}) of Cu(II) versus the milligram of Cu(II) adsorbed per gram of phase (Figure 7). From the adsorption isotherm study, the adsorption capacity of LC3 for Cu(II) was determined to be 207.17 mgg^{-1} which is higher than those previously reported for Cu(II) in other studies (5.2 [45], 12.0 [46], 66.7 [47], 73.5 [48], 110.5 [49], and 160.1 mgg^{-1} [50]). For comparison with the adsorption capacity of LC3 toward Cu(II), the Cu(II) adsorption capacity on the unmodified DEAE cellulose was evaluated and estimated to be 66.67 mgg^{-1} under the same batch conditions as well as LC3, as displayed in Figure 7. This provides that the adsorption capacity of Cu(II) was improved by 211% with the LC3 nanocomposites as compared to that with the unmodified DEAE cellulose.

Effect of shaking time

The shaking time effect is considered to be a principal factor when the static technique is exercised for the determination of adsorption capacity values of the metal ion. In this report, the shaking times within 5 to 120 min were investigated to attain the effect of contact time on Cu(II) adsorption. Results indicated fast equilibrium kinetics of Cu(II) adsorption on the surface of LC3 (Figure 8). It was found that over 200 mgg^{-1} Cu(II) was adsorbed onto the surface of LC3 within 20 min. However, after 20 min, minor change in the adsorption of Cu(II) was observed, and the value rose up to the maximum value of 207.17 mgg^{-1} after 120 min. The uptake capacity of Cu(II) was also raised up to more than 204 mgg^{-1} after 50 min until the maximum adsorption of LC3 toward Cu(II) was reached after 120 min.

Effect of temperature

The effect of temperature on the adsorption of LC3 for Cu(II) was studied in order to determine thermodynamic parameters. In this study, the effect of temperature on the adsorption of 25.0 mg LC3 along with 25.0 mL of 5.0 mgL^{-1} Cu(II) solution was investigated at different temperatures, ranging from 298 to 338 K. The results showed that adsorption capacity increases with decrease in solution temperature. This elaborates exothermic nature of adsorption process. Thermodynamic parameters linked with adsorption process, such as change in free energy ($\Delta G°$, kJmol^{-1}), entropy ($\Delta S°$, Jmol^{-1} K^{-1}), and enthalpy ($\Delta H°$, kJmol^{-1}), were calculated by employing the following equations:

$$K_d = (C_o - C_e / C_e) \times (V/m) \tag{1}$$

$$\ln K_d = \Delta S°/R - (\Delta H°/RT) \tag{2}$$

$$\Delta G° = -RT \ln K_d \tag{3}$$

where K_d is distribution adsorption coefficient, C_o and C_e denote initial and final concentrations of the metal before and after adsorption, respectively, V corresponds to the volume (mL), m represents the weight of the phase (g), R is the universal gas constant (8.314 Jmol^{-1} K^{-1}), and T corresponds to the temperature in Kelvin.

Table 2 Langmuir and Freundlich adsorption isotherm parameters for the adsorption of Cu(II) on LC3 phase

Langmuir model			Freundlich model		
Q_o (mgg^{-1})	b (Lmg^{-1})	R^2	K_f (mgg^{-1})	$1/n$	R^2
207.46	0.04	0.977	359.66	0.42	0.9203
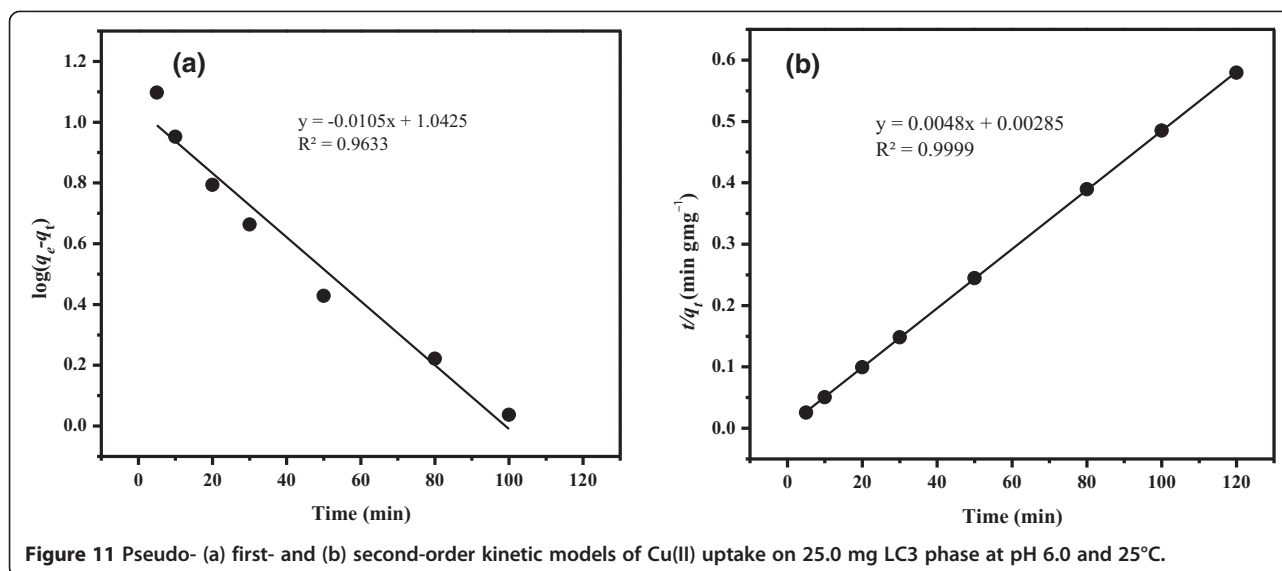
Figure 11 Pseudo- (a) first- and (b) second-order kinetic models of Cu(II) uptake on 25.0 mg LC3 phase at pH 6.0 and 25°C.

Thermodynamic parameters of $\Delta H°$ and $\Delta S°$ were calculated using Equation 2 from the slope and intercept of the linear variation of ln K_d with the reciprocal of the temperature (1/T), as displayed in Figure 9 and Table 1. The standard Gibbs free energy change, ΔG, was obtained from Equation 3 (Table 1). As can be depicted from Table 1, calculated thermodynamic parameters were all negative. The observed negative $\Delta H°$ value (-57.82 kJmol^{-1}) supports that the adsorption process of LC3 toward Cu(II) is exothermic in nature. The negative $\Delta S°$ value (-86.68 Jmol^{-1} K^{-1}) provides that the system randomness decreases during the adsorption process on the adsorbent surface, a general observation in most of the processes of metal ion uptake [49,50]. Finally, negative values of $\Delta G°$ suggest that the adsorption mechanism of LC3 toward Cu(II) is a generally spontaneous process and thermodynamically favorable.

Adsorption isotherm models

The adsorption isotherm analysis is very crucial to obtain an equation that accurately corresponds to the results. The obtained adsorption isotherm data for Cu(II) is therefore assessed by two well-known adsorption isotherm models, Langmuir and Freundlich. These two models were utilized to match the equilibrium data and acquire the correlation coefficient (R^2) values to assess fitting parameters. The Langmuir model describes a monolayer

adsorption phenomenon onto a completely homogeneous surface with equally available identical adsorption sites along with negligible interaction of adsorbed species. It can be defined by the following equation [51]:

$$C_e/q_e = (C_e/Q_o) + 1/Q_o b \qquad (4)$$

where C_e is the concentration of un-retained metal ion remaining in the filtrate at equilibrium (mg mL^{-1}) and q_e corresponds to the amount of adsorbed metal ion on adsorbent (mgg^{-1}). The symbols Q_o and b refer to Langmuir constants related to the maximum adsorption capacity (mgg^{-1}) and affinity parameter (Lmg^{-1}), respectively. Langmuir constants can be calculated from a linear plot of C_e/q_e against C_e with a slope and intercept equal to $1/Q_o$ and $1/Q_o b$, respectively. Moreover, a dimensionless constant separation factor or equilibrium parameter R_L is an additional characteristic of the Langmuir model, which is defined by the given equation below:

$$R_L = 1/(1 + bC_o) \qquad (5)$$

where b is the Langmuir constant, indicating the nature of adsorption and the shape of the isotherm and C_o is the initial concentration of the analyte of interest. The R_L values specify the type of isotherm, and R_L values within 0 to 1 suggest a favorable adsorption [52].

Table 3 Pseudo-first- and second-order kinetic model parameters for extraction of Cu(II) by LC3 phase

C_0 (mg/L)	$q_{e, exp}$ (mg/g)	Pseudo-first-order kinetic model			Pseudo-second-order kinetic model		
		k_1 (min^{-1})	$q_{e, cal}$ (mgg^{-1})	R^2	k_2 (gmg^{-1} min^{-1})	$q_{e, cal}$ (mgg^{-1})	R^2
400	207.17	2.42E-02	11.03	0.9633	0.01	207.58	0.999

Table 4 Uptake capacities and distribution coefficient values of different metal ions against unmodified DEAE cellulose and modified cellulose phases at pH 6.0 and 25°C

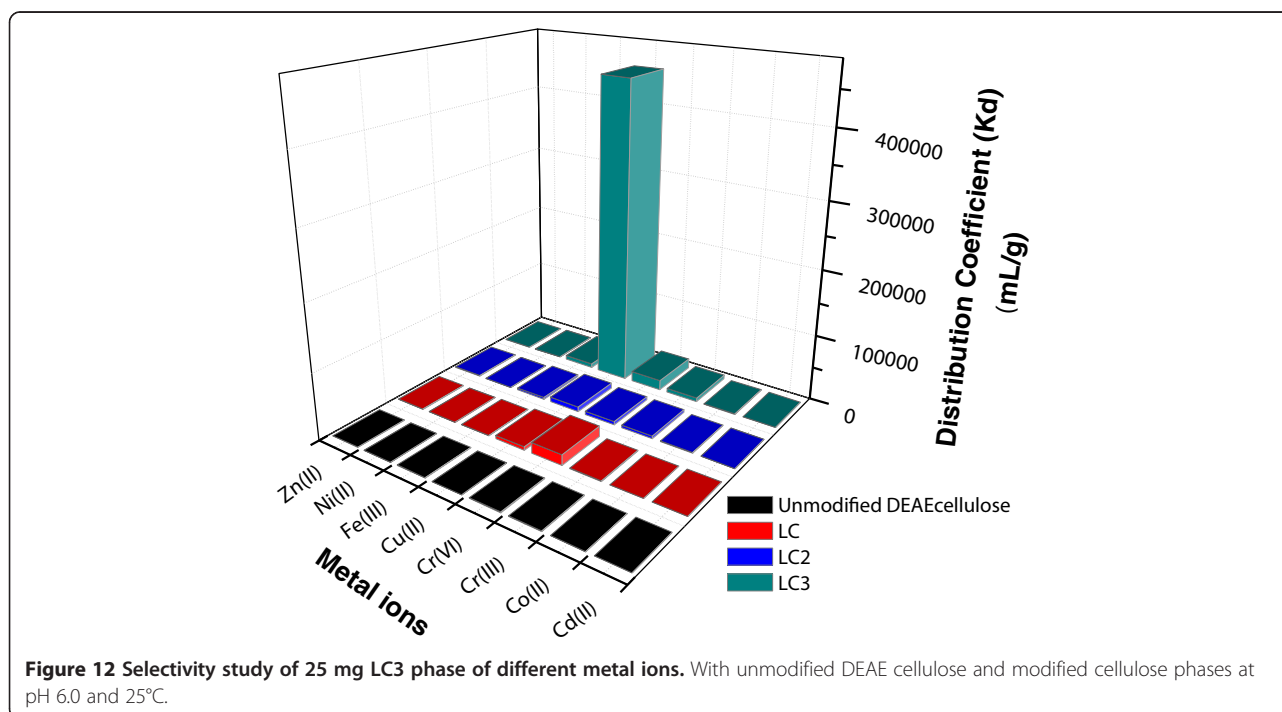| Metal ions	Unmodified DEAE cellulose		LC		LC2		LC3	
	q_e (mgg^{-1})	K_d (mLg^{-1})	q_e (mgg^{-1})	K_d (mLg^{-1})	q_e (mgg^{-1})	K_d (mLg^{-1})	q_e (mgg^{-1})	K_d (mLg^{-1})
Cd(II)	0.62	1.42×10^2	0.75	1.76×10^2	0.00	0.00	0.92	2.24×10^2
Co(II)	0.73	1.71×10^2	0.73	1.70×10^2	1.90	6.15×10^2	1.86	5.93×10^2
Cr(III)	2.33	8.70×10^2	2.15	7.53×10^2	4.01	4.07×10^3	4.27	5.88×10^3
Cr(VI)	2.46	9.67×10^2	4.71	1.61×10^4	4.14	4.83×10^3	4.69	1.51×10^4
Cu(II)	0.18	3.78×10^1	4.17	5.01×10^3	4.42	7.68×10^3	4.99	4.54×10^5
Fe(III)	2.37	8.98×10^2	2.03	6.85×10^2	3.76	3.02×10^3	4.29	6.02×10^3
Ni(II)	0.26	5.46×10^1	0.27	5.69×10^1	0.00	0.00	0.48	1.05×10^2
Zn(II)	0.81	1.92×10^2	0.84	2.03×10^2	2.19	7.79×10^2	1.09	2.79×10^2

On the other hand, Freundlich isotherm model is based on the assumption of a reversible adsorption process at multilayers on heterogeneous surface of the phase. It can be expressed by the following equation:

$$\log q_e = \log K_f + 1/n \ \log C_e \qquad (6)$$

where K_f and n are the Freundlich isotherm constants related to adsorption capacity and intensity of adsorption, respectively. Freundlich constants (K_f and n) can be calculated from the intercept and slope, respectively, of the linear plot of $\log q_e$ versus $\log C_e$.

By employing least square fit method, linear plots of Langmuir and Freundlich isotherm models were obtained (Figure 10). Table 2 represents values acquired from these models. From Table 2, it can be seen clearly that Langmuir model is better fitted as compare to Freundlich model. Langmuir model has higher correlation factor ($R^2 = 0.9737$) and close Q_0 value (207.46 mgg^{-1}) to that (207.17 mgg^{-1}) experimentally obtained from adsorption isotherm study. However, the correlation factor obtained from Freundlich model is less (0.9203) than that obtained from Langmuir model. In addition, the K_f value 359.66 mgg^{-1} represents large deviation from that obtained from the adsorption isotherm study. Considering these results, it can be concluded that a monolayer adsorption took place on the surface of adsorbent with homogenous adsorption sites. The R_L value of

Figure 12 Selectivity study of 25 mg LC3 phase of different metal ions. With unmodified DEAE cellulose and modified cellulose phases at pH 6.0 and 25°C.

Table 5 Determination of Cu(II) at different concentrations in real water samples utilizing LC3 phase

Environmental samples	Added (mgL^{-1})	Un-adsorbed (mgL^{-1})	Percentage extraction
Tap water	2.0	0.05	97.29
	10.0	0.47	95.26
	50.0	4.35	91.31
Ground water	2.0	0.04	98.23
	10.0	0.40	95.99
	50.0	3.86	92.27
Seawater	2.0	0.06	97.05
	10.0	0.67	93.26
	50.0	4.45	91.11
Wastewater	2.0	0.09	95.73
	10.0	0.67	93.26
	50.0	5.06	89.87

Cu(II) adsorption on the LC3 is 0.06, validating a favorable adsorption process based on the Langmuir model.

Kinetic models

Different kinetic models were studied in order to explore inherent kinetic adsorption parameters. These models are applied in order to check fitness of the experimental data, where correlation coefficient (R^2) value is taken as the measure of agreement between the experimental data. In this study, two kinetic adsorption models were

evaluated. The equation for pseudo-first-order adsorption kinetic can be expressed as follows:

$$\log(q_e - q_t) = \log q_e - (k_1/2.303)t \qquad (7)$$

where q_e (mgg^{-1}) and q_t (mgg^{-1}) are the amounts of adsorption at equilibrium and at time t (min), respectively, and k_1 denotes the adsorption rate constant of pseudo-first-order adsorption (min^{-1}). The adsorption rate constant k_1 and the adsorption capacity q_e were calculated from the slope and intercept of the plot of $\log(q_e - q_t)$ against t and found to be 2.42×10^{-2} min^{-1} and 11.03 mgg^{-1}, respectively, as illustrated in Figure 11a. In addition, the kinetic equation for pseudo-second-order adsorption can be written as follows:

$$t/q_t = 1/v_o + (1/q_e)t \qquad (8)$$

where $v_o = k_2$ is the initial adsorption rate (mgg^{-1} min^{-1}) where k_2 (gmg^{-1} min^{-1}) corresponds to the rate constant of the pseudo-second-order adsorption, q_e (mgg^{-1}) is the amount of metal ion adsorbed at equilibrium, and q_t (mgg^{-1}) refers to the amount of metal ion on the adsorbent surface at any time t (min). The plot of t/q_t versus t was developed in order to deduce kinetic parameters of v_o and q_e from the intercept and slope, respectively.

The correlation coefficient factor (R^2) obtained from pseudo-second-order plot was found to be 0.9999 (Figure 11b). Kinetic parameters v_o and q_e were found
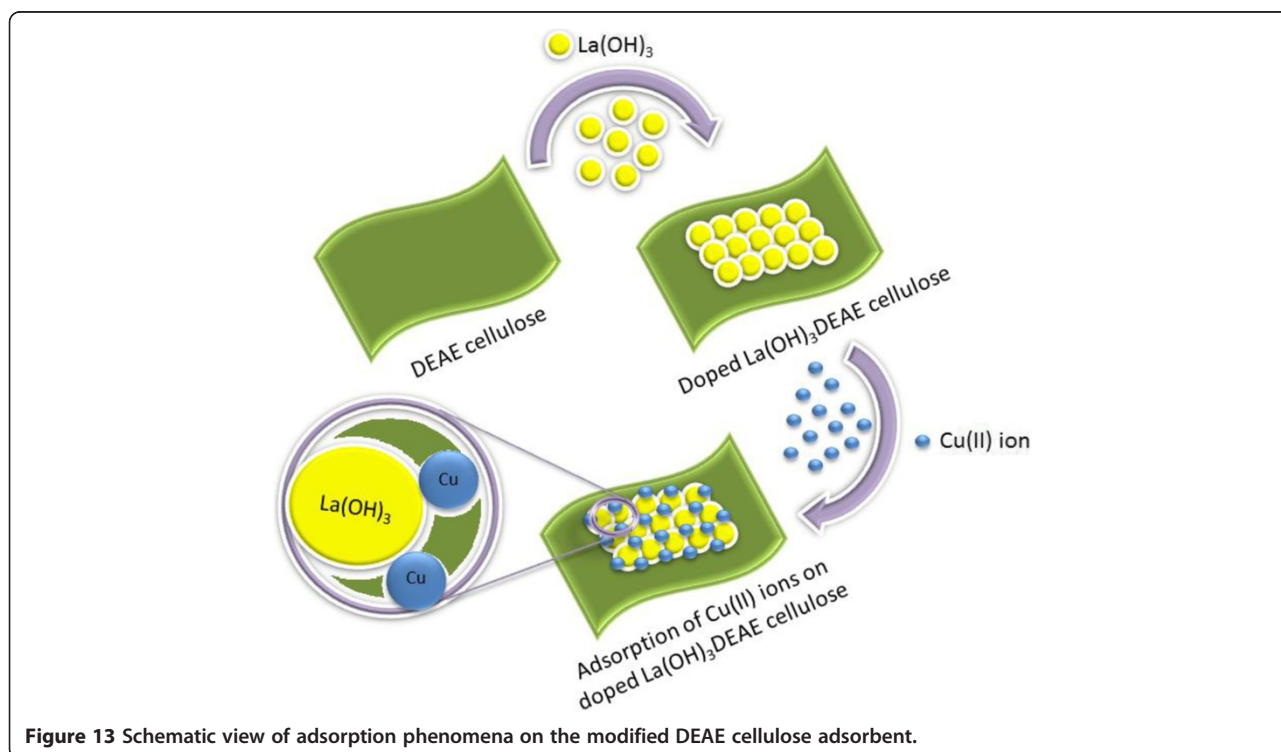
Figure 13 Schematic view of adsorption phenomena on the modified DEAE cellulose adsorbent.

to be 350.51 mgg^{-1} min^{-1} and 207.58 mgg^{-1}, respectively, and k_2 was estimated to be 0.01 gmg^{-1} min^{-1} for LC3 adsorption for Cu(II) (Table 3). It can be noticeably observed that the value of q_e obtained from the pseudo-second-order kinetic model is consistent with the outcome of adsorption isotherms, strongly supporting the validity of pseudo-second-order kinetic model.

Performance of proposed method
Selectivity studies
Selectivity studies of modified and unmodified DEAE cellulose adsorbents toward different metal ions, including Cd(II), Co(II), Cu(II),Cr(III), Cr(VI), Fe(III), Ni(II), and Zn(II), were investigated by determining the distribution coefficient of all the phases at optimum pH value (pH 6.0). Distribution coefficient (K_d) values were determined from Equation 1.

The values of distribution coefficient along with uptake capacities for all metal ions against different phases of cellulose at optimum pH 6.0 are summarized in Table 4. It can be clearly observed from Table 4 and Figure 12 that the Cu(II) adsorption on LC3 phase has the highest distribution coefficient value (4.54×10^5 mLg^{-1}). These results suggested that Cu(II) had the highest selectivity among all the metal ions and specifically toward the LC3 phase. However, the minimum overall value of K_d is observed in case of Cu(II) adsorption on the unmodified DEAE cellulose. Consequently, the modified phase LC3 provided the best selectivity for the separation of Cu(II) in this study.

Application in real environmental samples
The proposed method was applied to real environmental water samples for the extraction of Cu(II) using LC3 phase as an adsorbent. Four different water samples, including tap water, ground water, seawater, and wastewater, were collected from Jeddah, Saudi Arabia. These samples were spiked with Cu(II) and utilized for adsorption experiments with LC3 phase. These samples were studied under the same batch conditions at optimum pH 6.0. The percentage extraction of Cu(II) from these real samples was calculated and reported in Table 5. The results showed that the extraction of spiked Cu(II) water samples using LC3 phase in the range of 89.87% to 98.23%. Thus, these results were satisfactory, and the proposed method is reliable, feasible, and applicable to real sample analysis.

Conclusions
Nanocomposites of surface modified cellulose matrix were prepared successfully by growing different percentages of $La(OH)_3$ on DEAE cellulose surface. The morphology of these nanocomposites was confirmed by FE-SEM, EDS, XRD, FT-IR, and XPS. The analytical potential of newly synthesized nanocomposites for selective adsorption and determination of Cu(II) was evaluated. The outcome of the research revealed that among the different percentages of doped $La(OH)_3$ phases, the 10% doped $La(OH)_3$ phase (LC3) showed significant uptake capacity of Cu(II) in aqueous medium (Figure 13). LC3 phase also presented an excellent sensitivity toward Cu(II) adsorption and achieved good static uptake capacity. About 211% increase in adsorption capacity was achieved by LC3 phase as compared to unmodified DEAE cellulose. Adsorption data were found to be well fitted with the Langmuir isotherm model and followed second-order kinetic. Furthermore, the proposed method was applied to real environmental water samples and achieved adequate results for the extraction of Cu(II). Consequently, the method may display substantial promise for applying it as an applicable approach for a selective separation and detection of Cu(II) in complex matrices.

References
1. Hao Y-M, Man C, Hu Z-B: **Effective removal of Cu (II) ions from aqueous solution by amino-functionalized magnetic nanoparticles.** *J Hazard Mater* 2010, **184**:392–399.
2. Malkoc E, Nuhoglu Y: **Investigations of nickel (II) removal from aqueous solutions using tea factory waste.** *J Hazard Mater* 2005, **127**:120–128.
3. Northcott KA, Miyakawa K, Oshima S, Komatsu Y, Perera JM, Stevens GW: **The adsorption of divalent metal cations on mesoporous silicate MCM-41.** *Chem Eng J* 2010, **157**:25–28.
4. Hasan SH, Srivastava P: **Batch and continuous biosorption of Cu^{2+} by immobilized biomass of Arthrobacter sp.** *J Environ Manag* 2009, **90**:3313–3321.
5. Xue X, Li F: **Removal of Cu (II) from aqueous solution by adsorption onto functionalized SBA-16 mesoporous silica.** *Microporous Mesoporous Mater* 2008, **116**:116–122.
6. Lam KF, Yeung KL, McKay G: **A rational approach in the design of selective mesoporous adsorbents.** *Langmuir* 2006, **22**:9632–9641.
7. Jeong E-Y, Ansari MB, Mo Y-H, Park S-E: **Removal of Cu (II) from water by tetrakis (4-carboxyphenyl) porphyrin-functionalized mesoporous silica.** *J Hazard Mater* 2011, **185**:1311–1317.
8. Wang Y, Huang S, Kang S, Zhang C, Li X: **Low-cost route for synthesis of mesoporous silica materials with high silanol groups and their application for Cu (II) removal.** *Mater Chem Phys* 2012, **132**:1053–1059.
9. Zhang L, Yu C, Zhao W, Hua Z, Chen H, Li L, Shi J: **Preparation of multi-amine-grafted mesoporous silicas and their application to heavy metal ions adsorption.** *J Non-Cryst Solids* 2007, **353**:4055–4061.
10. Chakraborty S, Tare V: **Role of various parameters in synthesis of insoluble agrobased xanthates for removal of copper from wastewater.** *Bioresour Technol* 2006, **97**:2407–2413.

11. Kumar GP, Kumar P, Chakraborty S, Ray M: Uptake and desorption of copper ion using functionalized polymer coated silica gel in aqueous environment. *Sep Purif Technol* 2007, **57**:47–56.

12. Li J, Miao X, Hao Y, Zhao J, Sun X, Wang L: Synthesis, amino-functionalization of mesoporous silica and its adsorption of Cr (VI). *J Colloid Interface Sci* 2008, **318**:309–314.

13. Nasu A, Yamaguchi S, Sekine T: Solvent extraction of copper(I) and (II) as thiocyanate complexes with tetrabutylammonium ions into chloroform and with trioctylphosphine oxide into hexane. *Anal Sci* 1997, **13**:903–911.

14. Tao GH, Fang Z: Dual stage preconcentration system for flame atomic absorption spectrometry using flow injection on-line ion-exchange followed by solvent extraction. *J Anal Chem* 1998, **360**:156–160.

15. Soylak M, Erdogan ND: Copper(ii)-rubeanic acid coprecipitation system for separation-preconcentration of trace metal ions in environmental samples for their flame atomic absorption spectrometric determinations. *J Hazard Mater* 2006, **137**:1035–1041.

16. Manzoori JL, Abdolmohammad-Zadeh H, Amjadi M: Simplified cloud point extraction for the preconcentration of ultra-trace amounts of gold prior to determination by electrothermal atomic absorption spectrometry. *Microchim Acta* 2007, **159**:71–78.

17. Ahmed SA: Alumina physically loaded by thiosemicarbazide for selective preconcentration of mercury(ii) ion from natural water samples. *J Hazard Mater* 2008, **156**:521–529.

18. Alvarez AM, Alvarez JRE, Alvarez RP: Heavy metal analysis of rainwaters: a comparison of txrf and asv analytical capabilities. *J Radioanal Nucl Chem* 2007, **273**:427–433.

19. Soliman EM, Ahmed SA: Selective separation of silver(i) and mercury(ii) ions in natural water samples using alumina modified thiouracil derivatives as new solid phase extractors. *Int J Environ Anal Chem* 2009, **89**:389–406.

20. Pei S, Fang Z: Flame atomic absorption spectrometric determination of silver in geological materials using a flow-injection system with on-line preconcentration by coprecipitation with diethyldithio-carbamate. *Anal Chim Acta* 1994, **294**:185–193.

21. Saraji M, Yousefi H: Selective solid-phase extraction of Ni(II) by an ion-imprinted polymer from water samples. *J Hazard Mater* 2009, **167**:1152–1157.

22. Gustavo Rocha de C, Ilton Luiz de A, Paulo dos Santos R: Synthesis, characterization and determination of the metal ions adsorption capacity of cellulose modified with p-aminobenzoic groups. *Journal of Materials Research* 2004, **7**:329–334.

23. Mahmoud ME, Kenawy IMM, Soliman EM, Hafez MA, Akl MAA, Lashein RRA: Selective preconcentration of uranyl ion by silica gel phases modified with chelating compounds as inorganic polymeric ion exchangers. *Anal Sci* 2008, **24**:381–387.

24. Sato S, Yoshihara K, Moriyama K, Machida M, Tatsumoto H: Influence of activated carbon surface acidity on adsorption of heavy metal ions and aromatics from aqueous solution. *Appl Surf Sci* 2007, **253**:8554–8559.

25. Sanchez-polo M, Rivera-utrilla J: Adsorbent-adsorbate interactions in the adsorption of Cd(ii) and Hg(ii) on ozonized activated carbons. *Environ Sci Technol* 2002, **36**:3850–3854.

26. Clasen C, Kulicke W-M: Determination of viscoelastic and rheo-optical material functions of water-soluble cellulose derivatives. *Prog Polym Sci* 2001, **26**:1839–1919.

27. O'Connell DW, Birkinshaw C, O'Dwyer TF: Heavy metal adsorbents prepared from the modification of cellulose: a review. *Bioresour Technol* 2008, **99**:6709–6724.

28. Kaplan DL: *Biopolymers from renewable resources*. New York: Springer; 1998.

29. Kirk R, Othmer D: *Cellulose encyclopedia of chemical technology*. New York: Wiley; 1967.

30. Ishimura D, Morimoto Y, Saito H: Influences of chemical modifications on the mechanical strength of cellulose beads. *Cellulose* 1998, **5**:135–151.

31. Khan SB, Alamry KA, Marwani HM, Asiri AM, Rahman MM: Synthesis and environmental applications of cellulose/ZrO$_2$ nanohybrid as a selective adsorbent for nickel ion. *Composites Part B: Engineering* 2013, **50**:253–258.

32. Asiri AM, Khan SB, Alamry KA, Marwani HM, Rahman MM: Growth of Mn$_3$O$_4$ on cellulose matrix: nanohybrid as a solid phase adsorbent for trivalent chromium. *Applied Surface Science* 2013, **270**:539–544.

33. Ajtony Z, Bencs L, Haraszi R, Jeno S, Szoboszlai N: Study on the simultaneous determination of some essential and toxic trace elements in honey by multi-element graphite furnace atomic absorption spectrometry. *Talanta* 2007, **71**:683–690.

34. Montes-Bayon M, Pröfrock D, Sanz-Medel A, Prange A: Direct comparison of capillary electrophoresis and capillary liquid chromatography hyphenated to collision-cell inductively coupled plasma mass spectrometry for the investigation of Cd-, Cu- and Zn-containing metalloproteins. *J Chromatogr A* 2006, **1114**:138–144.

35. Li Z, Chang X, Zou X, Zhu X, Nie R, Hu Z, Li R: Chemically-modified activated carbon with ethylenediamine for selective solid-phase extraction and preconcentration of metal ions. *Anal Chim Acta* 2009, **632**:272–277.

36. Gao R, Hu Z, Chang X, He Q, Zhang L, Tu Z, Shi J: Chemically modified activated carbon with 1-acylthiosemicarbazide for selective solid-phase extraction and preconcentration of trace Cu(II), Hg(II) and Pb(II) from water samples. *J Hazard Mater* 2009, **172**:324–329.

37. Bonfil Y, Kirowa-Eisner E: Determination of nanomolar concentrations of lead and cadmium by anodic-stripping voltammetry at the silver electrode. *Anal Chim Acta* 2002, **457**:285–296.

38. Tanikkul S, Jakmunee J, Lapanantnoppakhun S, Rayanakorn M, Sooksamiti P, Synovec RE, Christian GD, Grudpan K: Flow injection invalve mini-column pretreatment combined with ion chromatography for cadmium, lead and zinc determination. *Talanta* 2004, **64**:1241–1246.

39. Ci L, Wei B, Xu C, Liang J, Wu D, Xie S, Zhou W, Li Y, Liu Z, Tang D: Crystallization behavior of the amorphous carbon nanotubes prepared by the CVD method. *J Cryst Growth* 2001, **233**:823–828.

40. Salavati-Niasari M, Hosseinzadeh G, Davar F: Synthesis of lanthanum hydroxide and lanthanum oxide nanoparticles by sonochemical method. *J Alloys Compd* 2011, **509**:4098–4103.

41. Peng F, Ren J-L, Xu F, Bian J, Peng P, Sun R-C: Comparative studies on the physico-chemical properties of hemicelluloses obtained by DEAE-cellulose-52 chromatography from sugarcane bagasse. *Food Res Int* 2010, **43**:683–693.

42. Strohmeier BR, Levden DE, Field RS, Hercules DM: Surface spectroscopic characterization of CuAl2O3 catalysts. *J Catal* 1985, **94**:514–530.

43. Pang Y, Zeng G, Tang L, Zhang Y, Liu Y, Lei X, Li Z, Zhang J, Xie G: PEI-grafted magnetic porous powder for highly effective adsorption of heavy metal ions. *Desalination* 2011, **281**:278–284.

44. Feng Y, Gong J-L, Zeng G-M, Niu Q-Y, Zhang H-Y, Niu C-G, Deng J-H, Yan M: Adsorption of Cd (II) and Zn (II) from aqueous solutions using magnetic hydroxyapatite nanoparticles as adsorbents. *Chem Eng J* 2010, **162**:487–494.

45. Yılmaz V, Hazer O, Kartal S: Synthesis, characterization and application of a novel ion-imprinted polymer for selective solid phase extraction of copper (II) ions from high salt matrices prior to its determination by FAAS. *Talanta* 2013, **2013**:2013.

46. Lan S, Wu X, Li L, Li M, Guo F, Gan S: Synthesis and characterization of hyaluronic acid-supported magnetic microspheres for copper ions removal. *Colloids and Surfaces A: Physicochemical and Engineering Aspects* 2013, **425**:42–50.

47. Zhou L, Wang Y, Liu Z, Huang Q: Characteristics of equilibrium, kinetics studies for adsorption of Hg (II), Cu (II), and Ni (II) ions by thiourea-modified magnetic chitosan microspheres. *J Hazard Mater* 2009, **161**:995–1002.

48. Zhao X, Zhang G, Jia Q, Zhao C, Zhou W, Li W: Adsorption of Cu (II), Pb (II), Co (II), Ni (II), and Cd (II) from aqueous solution by poly (aryl ether ketone) containing pendant carboxyl groups (PEK-L): equilibrium, kinetics, and thermodynamics. *Chem Eng J* 2011, **171**:152–158.

49. Monier M, Nawar N, Abdel-Latif D: Preparation and characterization of chelating fibers based on natural wool for removal of Hg (II), Cu (II) and Co (II) metal ions from aqueous solutions. *J Hazard Mater* 2010, **184**:118–125.

50. Wang J, Xu L, Cheng C, Meng Y, Li A: Preparation of new chelating fiber with waste PET as adsorbent for fast removal of Cu^{2+} and Ni^{2+} from water: kinetic and equilibrium adsorption studies. *Chem Eng J* 2012, **193**:31–38.

51. Langmuir I: The constitution and fundamental properties of solids and liquids. *J Am Chem Soc* 1916, **38**:2221–2295.

52. Mckay G, Blair HS, Gardener JR: Adsorption of dyes on chitin-I: equilibrium studies. *J Appl Polym Sci* 1982, **27**:3043–3057.